GLL

SURFACE WATER AND GROUNDWATER QUALITY ASSESSMENT USING THE WQI METHOD AND HUMAN HEALTH RISK ASSESSMENT (HHR) IN THE LOWER SEYBOUSE (ANNABA PLAIN), NORTHEAST ALGERIA

Fenazi Bilal, Boucenna Fatih, Zeddouri Aziez

Summary

This study was carried out to investigate the current status of surface water and groundwater quality in Lower Seybouse and Annaba Plain, NE Algeria. 36 surface water and groundwater samples were collected in this area, and various physicochemical parameters were analysed. The quality of surface water and groundwater for drinking and the associated health risks were assessed using a Water Quality Index (WQI) and a Human Health Risk Assessment (HHRA) model. The results show that all samples are alkaline with the EC values ranging from 1139 to 5555 μS/cm. The ionic dominance pattern was in the order of $Na^+ > Mg^{2+} > Ca^{2+} > K^+$ for cations and $Cl^- > HCO_3^- > SO_4^{2-} > NO_3^-$ for anions, respectively. The dominant water types are SO_4-Cl-Ca-Mg and SO_4-Cl-Na, formed by dissolution of evaporative and carbonate-rich material. All samples are unsuitable for drinking, with 1 sample classified as poor (rank = 4) and 35 samples as extremely poor (rank = 5). These samples are mainly located near the Seybouse Wadi, which is a natural outlet for wastewater from human activities. The assessment of non-carcinogenic risk showed that the Hazard Index (HI) for males ranged from 0.12 to 1.01 with a mean of 0.30 and only one sample exceeded value 1. For females, the HI was between 0.16 and 1.28 for females, with a mean of 0.39. The risk for children was even higher, ranging from 0.41 to 3.28, with a mean of 1.03, suggesting that children are more vulnerable to water contamination. The Carcinogenic Risk (CR) values for Pb ranged from 10^{-3} to $8.6 \cdot 10^{-3}$, with a mean of $2.6 \cdot 10^{-3}$ for males, and between $1.4 \cdot 10^{-3}$ to 10^{-2}, with a mean of $3.3 \cdot 10^{-3}$ for females, while for children the CR values ranged from $3.5 \cdot 10^{-3}$ to $2.7 \cdot 10^{-3}$, with a mean of $8.4 \cdot 10^{-3}$, indicating that no possible CR from water drinking.

Keywords

1. Introduction

In this world, water is a unique and limited resource [Zakir et al. 2020, Sanou et al. 2022]. It is essential for human consumption, irrigation and industry [Bodrud-Doza et al. 2019, Rahman et al. 2022]. Access to drinking water is also a prerequisite for well-being, a fundamental right, and a critical aspect of good health protection programs

[Touré et al. 2019, Sanou et al. 2022]. The lower Seybouse experiences chronic pollution of surface water and groundwater due to rapid urbanization, and intense industrial and agricultural development. This pollution affects various water locations in the region and is mainly caused by inorganic salts, toxic metals, cations and anions of the elements [Khanoranga and Khalid 2019, Zhang et al. 2020]. In recent decades, high concentration of heavy metals in surface water and groundwater has become a serious problem for human health. Such high concentrations are a result of both natural processes (such as weathering and erosion of rocks) and anthropogenic activities (domestic, industrial-isation and wastewater irrigation) [Rezaei et al. 2019]. Assessment of surface water and groundwater quality as well as health risk assessment have been extensively researched worldwide, particularly in the USA, Canada, and China [Qiu 2010, Yu et al. 2011, Li et al. 2018c, Zhang et al. 2020, Davies 2009]. Many techniques have been employed by researchers to evaluate groundwater quality, among which are the Water Quality Index (WQI) [Chen et al. 2019, Zhang et al. 2020, Adimalla and Qian 2019] and the Human Health Risk Assessment (HHRA). These indexes allow us to evaluate the carcinogenic and non-carcinogenic risk to human health [Sanou et al. 2022, Rezaei et al. 2019, Zhang et al. 2020, Adimalla and Qian 2019, Rahman et al. 2022, He and Wu 2018].

The study area is located in northeastern Algeria and it is a part of the Annaba Plain. It is drained by the Seybouse river. It has been contaminated by various chemical compositions due to production processes and materials of the metal steel complex (galvanization, slag, lime, steel, etc.). Agriculture is popular in this region, because soil is considered suitable for absorbing any kind of pollution, including heavy metals, hydrocarbons, and organic matter. Industrial and urban discharges, as well as chemical fertilizers and pesticides have been so intense that in certain sectors, particularly at the lower Seybouse (the confluence of the two streams Seybouse and Meboudja) [Débieche 2002], the environment has become dangerous for the local fauna, flora, and human health. In this sector, the Seybouse river serves as an open sewage. Water, whether soft, salty, rainwater, groundwater, or surface water, can be contaminated by harmful materials. It can cause various diseases that have a seriously impact on both health and the physical environment [Messadi et al. 1999].

We can distinguish three main objectives of this study: 1) analysis of the hydrogeo-chemical characteristics and hydrochemical facies of surface water and groundwater samples; 2) assessment of the overall surface water and groundwater quality for drink-ing using the WQI and researching the possible sources of pollution by mapping spatial distribution of WQI values; 3) evaluation of the non-carcinogenic risks and carcino-genic risks of lead via drinking groundwater for males, females, and children.

2. Materials and methods

2.1. General settings

The plain of lower Seybouse constitutes part of Annaba Plain (NE Algeria). To the west it borders with Edough, the dominant massif of Annaba, to the north with the Mediterranean Sea, to the east with the swamps of Mekrada, with the lake of Fetzara to

the southwest, and with the eastern prolongation of the Numidian chain to the south (Fig. 1).
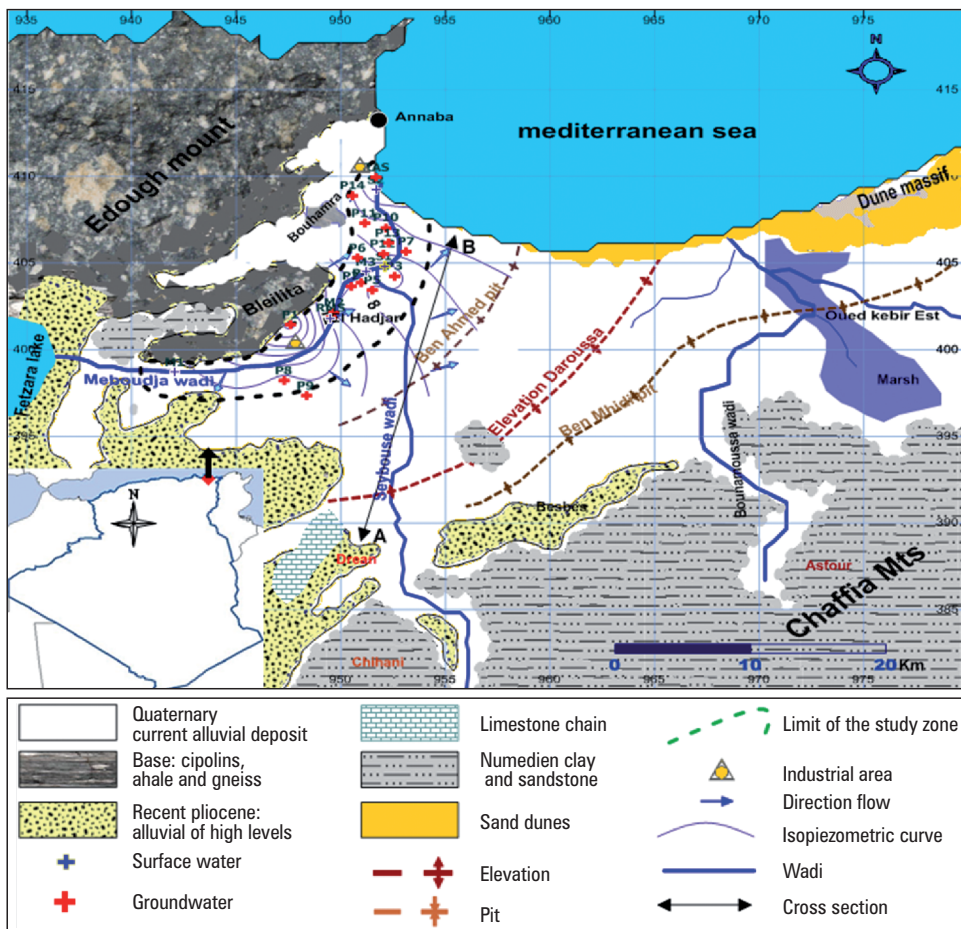
Source: Authors' own study

Fig. 1. Geographical map of the study area

The geology of the western boundary is characterised by the presence of a polycyclic metamorphic base covered by a Meso-Cenozoic tectonic roof and intersected by various magmatic rocks, such as: peraluminous leucogranites in the upper Burdigalian; sub-alkaline microgranites and peraluminous rhyolites in Langhien [Aissa et al. 1998]. To the south lie the alluvial deposits of Lake Fetzara and the Numidian chain of the Chaffia Mountains. To the southeast, the Numidian flysch was formed during the Oligocene. It is composed of thick sandstone with a content 90–97% of quartz. These layers of sandstone rest on pale clays, and both the sandstone and pale clays are covered

by supra-Numidian clays [Caby 1992] (Fig. 1). The structural study shows that the area is located in the Ben Ahmed pit, which is filled with sediments from the Mio-Plio-Quaternary age [Djabri et al. 2003]. The surface layer consists of sand-argillaceous formations including clay lenses that make the aquifer to be captive at certain points. The gravel-sand formations are located near the Seybouse river, adjacent to the outcrops of the Numidian sandstones. The substratum consists of compact grey clay.

The Seybouse drains a watershed of 6471 km^2 [Débieche 2002, Boucenna et al. 2018] and collects an enormous amount of pollution along its course. It joins the Meboudja stream in the Bouchet bridge area. The water supply of Meboudja stream is provided by the meteoric waters and the drainage of Lake Fetzara. On its flow path, the stream receives the urban waste (Hdjar Eddis, Sidi Amar, and el Hadjar) and the industrial effluents of the steel complex and industrial zone of Chaiba.

The region of Annaba is characterised by a Mediterranean climate with a dry and warm summer, and a mild and humid winter. The wet season lasts from October to April. The mean annual rainfall is around 650 mm/year, the average temperature is 19°C, the air humidity is around 70%, while the dominant wind directions are ENE and WNW. The hydrogeological study shows that the plain of Annaba consists of two superimposed aquifer horizons separated by an impermeable to permeable layer [Djidel 2004].

- Surface aquifer: based on the horizontal variation of the lithological facies, the shallow aquifer is composed of: altered gneiss, the dune system, and current alluvial deposits.

   In the present study we focus on the two following groundwater sites:

- The groundwater of the dune system limited by a coastal strip of wind dune sands, 0.5 to 5 m wide, and supplied directly by rainwater. It is exploited exclusively by wells for domestic usage, in particular, for drinking, breeding and irrigation of cultivation plots.

- The aquifer of the past and present alluvial deposits is located just behind the dune system towards the south. It is composed of past and current alluvial deposits with sandy clay, clay loam or sandy clay with some lenses of sand. It is important to note that the majority of the groundwater samples are collected from this zone.

2.2. Sampling and analysis

Samples of the groundwater and surface water in the study area were collected in November 2019, indicating a spatial variation in hydrogeochemical facies. A total of 36 samples were taken from the lower Seybouse plain. The samples were distributed as follows:

- 28 samples were taken from wells tapping into the surface water table,
- 5 samples were taken from Meboudja Wadi,
- 3 samples were taken from the Seybouse river,
- 1 sample is taken from industrial discharges (industrial unity of metal steel).

The measurements of pH and temperature were carried out in the field. The water samples were taken from 1000 ml polyethylene bottles with poly-sealing plugs for the major elements. Chemical analyses and isotopic measurements were run at the Laboratory of Radio-Analysis and Environment of the National School of Engineers of Sfax (Tunisia).

The major elements (Na^+, Mg^{2+}, Ca^{2+}, K^+, Cl^-, SO_4^{2-}, HCO_3^-, PO_4^{2-} and NO_3^-) were analysed by high performance ionic liquid chromatography (HPILC) equipped with I/Pak TM CM/D for cations, using EDTA and nitric acid as an elutint, and on a Metrohm chromatograph equipped with CI SUPER-SEP columns for anions, using phthalic acid and acetonitrile as an eluent. The overall detection limit for ions was 0.04 mg · L^{-1}. The concentrations of CO_3^{2-} and HCO_3^- were analysed in the laboratory by titration using 0.1 N HCl. The analytical accuracy was cross-checked by calculating Ionic Balance Error (IBE) as follows:

$$IBE = \frac{\sum cations - \sum anions}{\sum cations + \sum anions} \cdot 100\% \tag{1}$$

Where all cations and anions were expressed in meq · L^{-1}. The computed IBE was within the acceptable limit of ± 5%. In this study, the calculated results showed that the IBE for all samples was less than 5%.

2.3. Methods

Water quality index (WQI)

The Water Quality Index (WQI) is a useful tool for assessing the general quality of water [Adimalla et al. 2018c, Khan and Jhariya 2017]. In an effective way, it enables the perception of the water quality by condensing the vast amount of surface and groundwater quality data into a single value. The WQI is frequently used in various parts of the world to assess the suitability of drinking water [Adimalla and Qian 2019, Verma et al. 2018, Khan and Jhariya 2017, Wu et al. 2017]. For each of the water quality parameters, the first step is to calculate the weights of these parameters (Wi). The maximum weight is '5', and it is given for its significance in determining water quality, while the minimum weight – '2' – is given for its lesser significance. The second step is to assign each parameter a quality rating scale (Q_i). Finally, the WQI is determined by the following equations (2)–(5):

$$Wi = \frac{wi}{\sum_i^n Wi} \tag{2}$$

$$Q_i = \frac{C_i - C_{ip}}{S_I - C_{ip}} \cdot 100 \tag{3}$$

$$SI_i = Wi \cdot Q_i \tag{4}$$

$$WQI = \sum_{i=1}^{n} SI_i \tag{5}$$

where:
- Wi – the relative weight,
- wi – the weight of each parameter,
- n – the number of parameters,
- C_i – the concentration of each chemical parameter in each water sample,
- C_{ip} – the ideal value of the parameter in pure water (C_{ip} = 0 for all, except pH with C_{ip} = 7 and DO = 14.6 mg/L),
- S_I – the maximum allowable limit (MAL) [WHO 2017] value for each chemical parameter,
- SI_i – the sub-index of i-th parameter,
- Q_i – the quality rating scale based on concentration of i-th parameter.

The WQI values can be classified inon five categories: excellent, good, moderate, poor, and extremely poor (Table 1) [Li et al. 2010, Adimalla et al. 2018, Zotou et al. 2019, Zhang et al. 2020].

Table 1. Classification of surface water and groundwater based on the WQI values

WQI	Rank	Water quality
< 50	1	excellent
50–100	2	good
100–150	3	moderate
150–200	4	poor
> 200	5	very poor

Human Health Risk Assessment (HHRA) Model

The evaluation of health risks is crucial for the assessment of groundwater quality [Adimalla and Qian 2019, Chen et al. 2017, Adimalla 2018, Adimalla 2019]. To analyse the potential negative impacts of groundwater contamination on the health of both children and adult, the United States Environmental Protection Agency (USEPA) developed the human health risk assessment (HHRA) model [Zhang et al. 2020, Li et al. 2016c, 2019b, Adimalla et al. 2019, Adimalla and Qian 2019a, Adimalla and Wu 2019]. Drinking and bathing are the major ways through which human body absorbs harmful substances from groundwater [Adimalla and Qian 2019]. The HHRA includes non-carcinogenic risks and carcinogenic risks [Zhang et al. 2020]. The models for non-carcinogenic risks via ingestion and dermal contact are as follows [Zhang et al. 2020, Li et al. 2016c, Wu and Sun 2016, Adimalla et al. 2019]:

$$CDI = \frac{C \cdot IR \cdot EF \cdot ED}{BW \cdot AT} \tag{6}$$

$$HQ_{\text{oral}} = \frac{CDI}{RFD_{\text{oral}}} \tag{7}$$

The non-carcinogenic risk through dermal contact is expressed as [Li et al. 2017b]:

$$CDD = \frac{DA \cdot EV \cdot SA \cdot EF \cdot ED}{BW \cdot AT} \tag{8}$$

$$DA = K \cdot C \cdot t \cdot CF \tag{9}$$

$$SA = 239 \cdot H^{0.417} \cdot BW^{0.517} \tag{10}$$

$$HQ_{\text{dermal}} = \frac{CDD}{RFD_{\text{dermal}}} \tag{11}$$

$$RFD_{\text{dermal}} = RFD_{\text{oral}} \cdot ABS_{\text{gi}} \tag{12}$$

Hence, the total non-carcinogenic risks (hazard index HI) calculation is:

$$HI_j = HQ_{\text{oral}} + HQ_{\text{dermal}} \tag{13}$$

$$HI_{\text{total}} = \sum_{j=1}^{m} HI_j \tag{14}$$

where:
- *CDI* – chronic daily dose via ingestion (mg/kg day),
- *C* – concentration of pollutant for groundwater (mg $\cdot$ L^{-1}),
- *HQ*$_{\text{oral}}$ and *HQ*$_{\text{dermal}}$ – hazard quotient through oral and dermal exposure pathways,
- *CDD* – chronic daily dose via dermal contact (mg/kg day),
- *DA* – exposure dosage (mg $\cdot$ cm^{-2}), SA: skin surface area (cm^{-2}),
- *RFD*$_{\text{oral}}$ and *RFD*$_{\text{dermal}}$ – reference dosage via oral and dermal contact (mg/kg day),
- ABS$_{\text{gi}}$ – gastrointestinal absorption factor,
- *IR* – ingestion rate (L/d),
- *EF* – exposure frequency (d),
- *ED* – exposure duration (a),
- *BW* – average body weight (kg),
- *AT* – average time (d),
- *K* – skin permeability coefficient (cm/h),
- *t* – contact duration (h/d),
- *CF* – conversion factor,
- *H* – average height (cm),
- *EV* – exposure frequency (d).

The meanings and index values of other parameters are shown in Table 2.

The carcinogenic risk (CR) was estimated by multiplying the chronic daily dose via dermal contact (CDD) with the cancer slope factors (CSF) This risk is defined as the increased risk of developing cancer over the course of a lifetime due to exposure to a probable carcinogen [USEPA 1989, Tepanosyan et al. 2017, Sanou et al. 2022]:

$$CR = CDD \cdot CSF \qquad (15)$$

where:

CR – carcinogenic risk,
CDD – chronic daily dose via dermal contact (mg/kg day),
CSF – cancer slope factors (mg/kg/day).

According to USEPA [2010], Rais [2017], Mohammadi et al. [2019], Sanou et al. [2022], the admissible risk limit is 10^{6-}.

Table 2. Key parameters for computing the health risks through ingestion and dermal pathways

Parameters	Males	Females	Children	Units	Parameters	Males	Females	Children	Units
Ingestion rate (IR)	1.5	15	0.7	L/d	Skin permeability coefficient (K)	0.001			cm/h
Exposure frequency (EF)	365	365	365	d	Contact duration (t)	0.4			h/d
Exposure duration (ED)	30	30	12	a	Conversion factor (CF)	0.001			–
Average body weight (BW)	70	55	12	kg	Average height (H)	165.3	153.4	99.4	cm
Average time (AT)	10,950	10,950	4380	d	Exposure frequency (EV)	1			d

3. Results and discussion

3.1. Physicochemical data

Table 3 presents the statistical results of the water quality for the 36 surface water and groundwater samples. The pH values of the water samples were in the range of 7.02–8.16 (mean = 7.59), which falls within the acceptable pH range (6.5 to 8.5) and indicates that the water samples are alkaline. The EC values varied widely from 1139 to 5555 μS/cm, with a mean value of 2407.38 μS/cm. According to the WHO (2017), the Maximum Permissible Limit (MPL) of EC should be < 1500 μS/cm. Most water samples exceeded this limit, meaning that they are harmful to human health and tasteless. The ionic dominance pattern was in the order of $Na^+ > Mg^{2+} > Ca^{2+} > K^+$ for cations and $Cl^- > HCO_3^- > SO_4^{2-} > NO_3^-$ for anions. The concentrations of sodium and chloride were the highest among the cations and anions, respectively. A certain level of sodium is essential for maintaining human health, but its excessing consumption increases the

risk of diseases such as osteoporosis and hypertension [Zhang et al. 2020, Adimalla and Qian 2019a, Li et al. 2019a]. According to the WHO [2017], the Maximum Permissible Limit (MPL) for Na^+ should not exceed 61.11%. The health of humans also depends on Ca^{2+} and Mg^{2+}. A deficiency of Ca^{2+} in the body can cause various illnesses, such as stroke, osteoporosis, and colorectal cancer. Meanwhile, a high Mg^{2+} content has a laxative effect [WHO 2017, Adimalla and Qian 2019a, Zhang et al. 2020]. This study found that 97% of water samples met the maximum permissible limit for Ca^{2+}, and 61% for Mg^{2+}, while the K^+ concentration ranged from 3.4 to 30.15 mg/L, with 27.77% of samples remaining below the MPL. Furthermore, Chloride concentration ranged from 270.93 to 1609.28 mg/L, and 88.88% of water samples were within the upper limit ($\leq$ 600). The concentrations of HCO_3^- ranged from 238.31 to 603.61 mg/L. The SO_4^{2-} concentration in water samples from the study area varied between 85.93 and 642.57 mg/L, with 87.18% of samples below the MPL. The NO_3^- concentration in water samples ranged from 14.47 to 84.36 mg/L, with 69.44% of the water samples falling within the upper limit. In fact, a number of previous studies have found a strong link between agriculture and nitrate levels in groundwater and surface water [Debernardi et al. 2008, Adimalla 2018]. Nitrate levels above 50 mg/L can lead to such health issues as methemoglobinemia, stomach cancer, goiter, birth defects, and hypertension [Bao et al. 2017, Fan 2011].

The study area is an industrial zone, the Metal Steel Complex – El Hadjar. The primary non-carcinogenic and carcinogenic contaminant in the area is Pb. It has been classified as a toxic element due to its physical and behavioural effects on infants (who are more susceptible to it) compared to adults and young children [Environmental protection agency 2017]. Additionally, lead has a more severe impact on children's brains and nervous systems. In this study, the adopted Pb concentration range was from 0 to 0.193 mg/L. Therefore, based on this criterion, 35 water samples are not suitable for human consumption , and 35 water samples were deemed unsuitable, with 97.22% of all samples exceeding the upper limit. High concentration of Pb can be explained by wastewater discharges of the steel complex located near the wadi (0.193 mg/L). Consequently, the pollution from leads is the most serious in the study area. Additionally, the concentrations of Cu, Mn^{2+}, and Zn were all below their respective upper limits of 2, 0.4 and 3 mg/L respectively, whereas the concentration of 77.77% of Cr^{6+} in the samples was within the upper limit (0.05 mg/L).

Table 3. Statistical summary of chemical composition of groundwater in the study region

Parameters	Units	WHO (2017) MAL	Min	Max	Mean	Median	SD	P%
pH	–	8.5	7.02	8.16	7.592	7.61	0.277	100
EC	(uS/cm)	1500	1139	5555	2407.38	2275.5	827.96	94.44
K^+	mg/L	12	3.4	30.15	15.594	14.8	6.698	27.77

Table 3. cont.

Parameters	Units	WHO (2017) MAL	Min	Max	Mean	Median	SD	P%
Na^+	mg/L	200	110,93	667.88	233.488	197.53	129.055	61.11
Ca^{2+}	mg/L	200	62.6	415.25	111.908	96.82	66.356	97
Mg^{2+}	mg/L	150	31.14	316.59	144.634	147.64	70.392	61
HCO_3^-	mg/L	–	238.31	603.61	403.74	381.43	101.141	–
SO_4^{2-}	mg/L	400	85.93	642.57	258.896	222,85	114.173	87.18
Cl^-	mg/L	600	270.93	1609.28	509.074	387.43	313.683	88.88
PO_4^{3-}	mg/L	5	0.17	4.04	1.153	0.81	0.979	100
NO_3^-	mg/L	50	14.47	84.36	43.5326	46.57	19.8	69.44
DOC	mg/L	–	9.87	78.9	29.0211	23.1	16.594	–
DO	mg/L	5	1.4	3	2.29	2.4	0.46	100
Cr^{6+}	mg/L	0.05	0	0.092	0.047	0.0415	0.0223	77.77
Cu	mg/L	2	0	0.045	0.0236	0.02	0.0091	100
Fe	mg/L	-	0.084	1.028	0.214	0.1	0.253	–
Mn^{2+}	mg/L	0.4	0.027	0.103	0.0366	0.033	0.014	100
Pb	mg/L	0.01	0	0.193	0.058	0.0485	0.039	2.77
Zn	mg/L	3	0	0.046	0.026	0.02	0.01	100

MAL: Maximum allowable limit

P: Percentage of the sample below the permissible limits (MAL)

3.2. The dominant water types

The hydrochemical type of water samples are usually classified using the Piper diagram on the basis of major ions [Piper 1944, He and Li 2019, Li et al. 2016c, Xu et al. 2019a, Zhang et al. 2020]. Figure 3 shows that the cations of water samples in this study area were mainly plotted in zones C followed by B, indicating no dominant types and magnesium types of water. The anions were represented by zone B and G, indicating that the groundwater is mainly of the chloride type and no dominant type. Nearly all water samples were plotted in zone I, with only one sample in zone II, demonstrating that SO_4-Cl-Ca-Mg and SO_4-Cl-Na were the dominant water types. These hydrochemical types are mainly related to the dissolution of evaporate material found in the gypsum deposits and the dissolution of carbonate-rich material (limestone and dolomitic limestone of Triassic and Miocene outcrops).
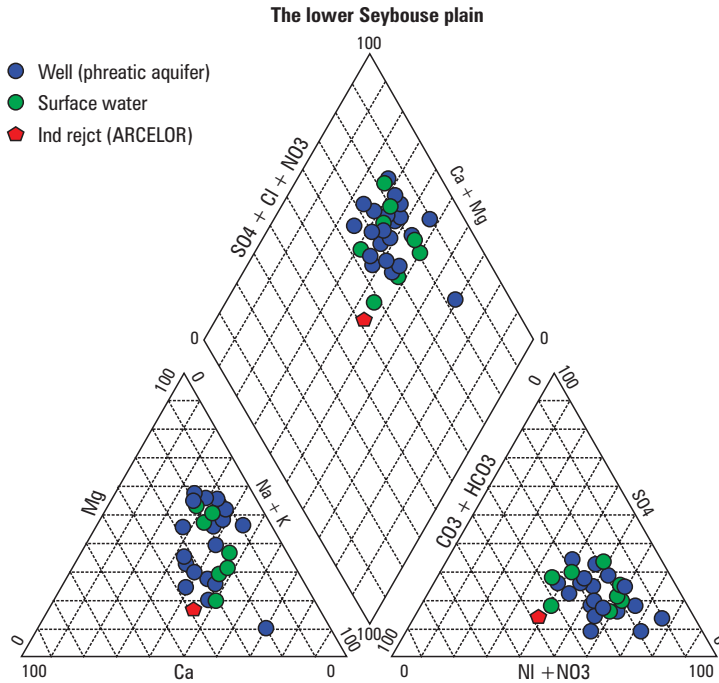
Source: Authors' own study

Fig. 2. Piper diagram of surface water and groundwater samples

3.3. Water quality index (WQI)

To evaluate and rank surface water and groundwater quality in this study area, the water quality index (WQI) was used. Table 4 shows the WQI values for all water samples.

**Table 4.** The WQI values and ranks for water samples

Numbers	WQI	Rank	Numbers	WQI	Rank	Numbers	WQI	Rank
M1	555.66	5	W4	465.95	5	W17	377.92	5
M2	561.18	5	W5	326.11	5	W18	360.82	5
M3	927.69	5	W6	788.81	5	W19	586.87	5
M4	1055	5	W7	428.12	5	W20	317.15	5
M5	752.65	5	W8	1480.28	5	W21	919.62	5
S1	604	5	W9	974.58	5	W22	725.1	5
S2	830.8	5	W11	608.3	5	W23	714.86	5

Table 4. cont.

Numbers	WQI	Rank	Numbers	WQI	Rank	Numbers	WQI	Rank
S3	705.24	5	W12	678.46	5	W24	183.05	4
R MS	1646.31	5	W13	361.44	5	W25	608.13	5
W1	515	5	W14	479.1	5	W26	446.25	5
W2	882.95	5	W15	634.12	5	W27	330.7	5
W3	554.65	5	W16	445.86	5	W28	370.26	5

According to Table 4, the WQI values range from 183.05 to 1646.31, with 35 samples ranked as extremely poor (rank = 5) and 1 sample ranked as poor (rank = 4). The evaluation results indicated that all surface water and groundwater samples were unsuitable for drinking water.

The spatial distribution of WQI is shown in Figure 3. As the map shows, the extremely poor surface water and groundwater samples are mainly located near the Wadi, which is a natural outlet of wastewater from human activities (domestic and industrial) and to a lesser extent from agriculture. In addition, one sample of groundwater was classed as poor in a location relatively far from any industrial area.
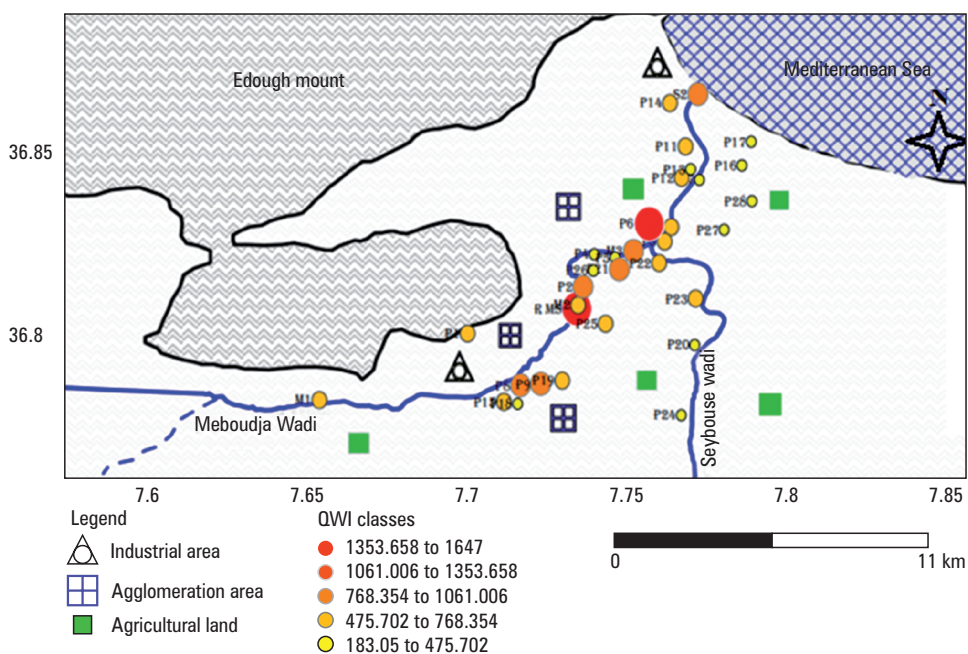
Source: Authors' own study

Fig. 3. Spatial distribution of WQI in the study area

3.4. Human Health Risk Assessment

Non-carcinogenic Risk (HI) Assessment of Lead

The most efficient method for determining the non-carcinogenic health risk in different age groups is the health risk assessment (HRA) model [Zhang et al. 2020, Li et al. 2016c, 2019b, Adimalla and Qian 2019a, b]. As discussed earlier, 96% of the groundwater samples exceeded the Maximum Allowable Limit (MAL) for Pb. Therefore, it is crucial to evaluate the risk to human health from excessive lead and nitrate intake for various age groups living in the study area. The calculated results of hazard index (HI) for adults and children in this study area through oral intake and dermal contact are presented in Table 5. When HI >1, there is a high non-carcinogenic risk to health and if HI<1, there is no non-carcinogenic risk to health.

Table 5. Non-carcinogenic risk for children, females, and males in the study area

Samples	HI		
	Males	Females	Children
P1	0.29	0.36	0.93
P2	0.59	0.74	1.91
P3	0.3	0.38	0.97
P4	0.24	0.3	0.79
P5	0.12	0.16	0.41
P6	0.29	0.37	0.95
P7	0.2	0.26	0.66
P8	1.01	1.28	3.28
P9	0.61	0.77	1.97
P10	0.22	0.28	0.73
P11	0.33	0.42	1.08
P12	0.4	0.51	1.31
P13	0.15	0.19	0.5
P14	0.24	0.30	0.79
P15	0.34	0.43	1.1
P16	0.21	0.26	0.68
P17	0.18	0.23	0.6
P18	0.16	0.21	0.54
P19	0.30	0.39	1
P20	0.12	0.16	0.41

Table 4. cont.

Samples	HI		
	Males	Females	Children
P21	0.58	0.74	1.89
P22	0.31	0.39	1.02
P23	0.30	0.38	0.97
P24	0.18	0.23	0.6
P25	0.34	0.43	1.1
P26	0.22	0.28	0.73
P27	0.13	0.16	0.41
P28	0.16	0.21	0.54

The results of Health Risk Assessment (Table 5) show that the hazard index (HI) for children ranges from 0.41 to 3.28, with a mean value of 1.03. Ten samples (35.71%) of groundwater had the HI exceeding 1, which indicates that the Pb concentration for almost all groundwater samples poses little non-carcinogenic health risks to children. For male adults, the HI ranges from 0.12 to 1.01, with a mean of 0.30. Only one sample exceeded 1 HI, which means that most samples can pose little non-carcinogenic health risks. For female adults, the HI ranges from 0.16 to 1.28, with a mean equal to 0.39. As with male adults, only one sample exceeded 1, which also means that there is little non-carcinogenic health risk to female adults. We observed that the mean value of HI exceeded 1 for children, while or males and females adults the HI was lower than 1, indicating that mixing local groundwater can significantly decrease the non-carcinogenic hazards for adults, but it is not as effective in reducing the risks in the case of children.

Carcinogenic risk analysis

Some of heavy metals, such as lead (Pb), are carcinogenic and prolonged exposure to their low concentrations can increase the risk of cancer and other diseases [Cao et al. 2014, Sanou et al. 2022, Mohammadi et al. 2019]. In this study, we adopted Pb as an example of a carcinogen to evaluate carcinogenic risk for males, females and children. The results of carcinogenic risk (CR) values for Pb in the analysed samples in study area are presented in Figure 4. The CR values of Pb range from 10^{3-} to $8.6 \cdot 10^{-3}$ with mean of $2.6 \cdot 10^{-3}$ for males, and from $1.4 \cdot 10^{-3}$ to 10^{-2} with mean of $3.3 \cdot 10^{-3}$ for females, while for children the CR values range from $3.5 \cdot 10^{-3}$ to $2.7 \cdot 10^{-3}$ with mean of $8.4 \cdot 10^{-3}$. Due to high Pb concentration in groundwater samples, all these results for males, females and children are higher than $1 \cdot 10^{-6}$, pointing to some carcinogenic risks for adults (both males and females) and to high health hazard for children. Therefore, it is necessary to monitor the quality of groundwater with great attention, especially with regard to Pb.
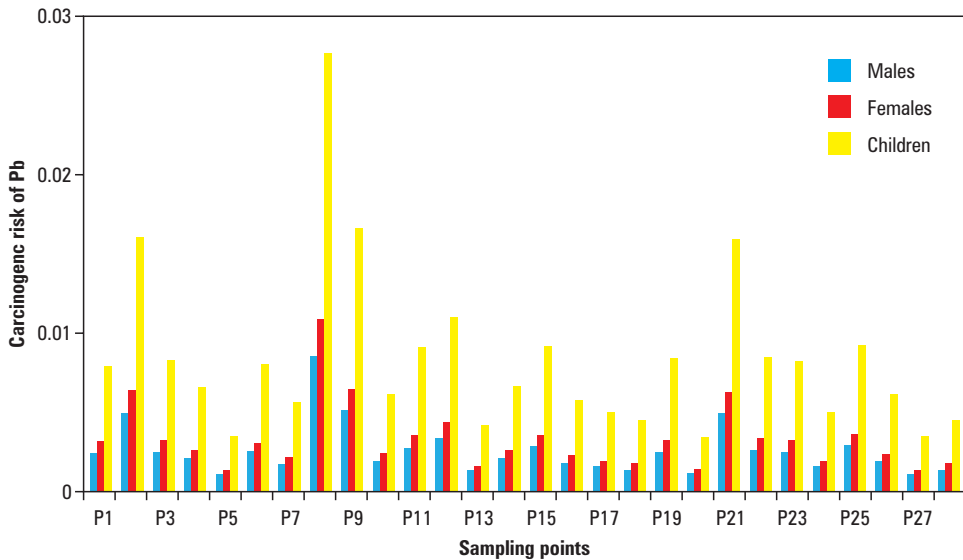
Source: Authors' own study

Fig. 4. Carcinogenic risk of Pb in study area

4. Conclusion

In this study, 36 surface water and groundwater samples were collected and analysed for physicochemical parameters and heavy metals. Groundwater chemistry was delineated by the Piper diagram, and the WQI index method was used to evaluate the surface water and groundwater quality. Health risks, both non-carcinogenic and carcinogenic, related to drinking groundwater were assessed. The main conclusions of the study are as follows:

1. All of the surface water and groundwater samples are alkaline, and the EC values ranged from 1139 to 5555 μS/cm. The ionic dominance pattern was in the order of $Na^+ > Mg^{2+} > Ca^{2+} > K^+$ for cations and $Cl^- > HCO_3^- > SO_4^{2-} > NO_3^-$ for anions, respectively. The dominant water type is SO_4-Cl-Ca-Mg and SO_4-Cl-Na. The processes of the dissolution of evaporate material present in the gypsum deposits and the dissolution of carbonate-rich material were observed.

2. As reported by the water quality index (WQI), all surface water and groundwater samples are unsuitable for drinking, with 1 sample ranked as poor (rank = 4) and 35 samples ranked as extremely poor (rank = 5). These samples are mainly located near the Seybouse Wadi, which serves as a natural outlet of wastewater from human activities (domestic and industrial).

3. The assessment of non-carcinogenic risk showed that the hazard index (HI) for males ranged from 0.12 to 1.01, with a mean of 0.30. Only one sample exceeded 1.

For females the HI is between 0.16 and 1.28, with a mean of 0.39. Unfortunately, the risk for children was even greater, ranging from 0.41 to 3.28, with a mean of 1.03, proving that children are more vulnerable to water contamination.

4. In relation to the carcinogenic risk, the CR values of Pb were found to be less than 10^{-6}. These values ranged from 10^{-3} to $8.6 \cdot 10^{-3}$, with a mean of $2.6 \cdot 10^{-3}$ for males, and between $1.4 \cdot 10^{-3}$ to 10^{-2}, with a mean of $3.3 \cdot 10^{-3}$ for females, while for children the CR values ranged from $3.5 \cdot 10^{-3}$ to $2.7 \cdot 10^{-3}$, with a mean of $8.4 \cdot 10^{-3}$, indicating that no possible CR from water drinking.

References

Adimalla N., Qian H. 2019b. Groundwater quality evaluation using water quality index (WQI) for drinking purposes and human health risk (HHR) assessment in an agricultural region of Nanganur, South India. Ecotoxicol Environ Saf., 176, 153–161.

Adimalla N., Qian H. 2019a. Hydrogeochemistry and fluoride contamination in the hard rock terrain of central Telangana, India: analyses of its spatial distribution and health risk. SN Appl. Sci., 1(3), 202.

Adimalla N., Wu J. 2019. Groundwater quality and associated health risks in a semi-arid region of South India: implication to sustainable groundwater management. Hum. Ecol. Risk Assess., 25(1–2), 191–216.

Adimalla N., Li P. 2018. Occurrence, health risks, and geochemical mechanisms of fluoride and nitrate in groundwater of the rock-dominant semi-arid region, Telangana State, India. Hum. Ecol. Risk Assess. Int. J. https://doi.org/10.1080/ 10807039.2018.1480353.

Adimalla N., Li P., Venkatayogi S. 2018c. Hydrogeochemical evaluation of groundwater quality for drinking and irrigation purposes and integrated interpretation with water quality index studies. Environ. Process., 5(2), 363–383. https://doi.org/10. 1007/s40710-018-0297-4.

Aissa Djamel Eddine et al. 1998. Géologie et métallogénie sommaire du massif de l'Edough Bulletin_SGN_V21-2. Mem. Serv. Geol., Algerie, 9, 7–55.

Bao Q., Hu W., Qi Y., Tang W., Wang P., Wan J., Chao X.J., Yang 2017. Nitrate reduction in water by aluminium alloys particles J. Environ. Manag., 196, 666–673.

Bodrud-Doza M., Bhuiyan M.A.H., Islam S.D.U., Quraishi S.B., Muhib M.I., Rakib M.A., Rahman M.S. 2019. Delineation of trace metals contamination in groundwater using geostatistical techniques: A study on Dhaka City of Bangladesh. Groundwaterfor Sustainable Development, 9, 100212.

Boucenna F., Djorfi S., Fenazi B. 2018. Geochemical and isotopic study of groundwater of anthropogenic coastal aquifer: Meboudja and Low seybouse Plain, Annaba (Ne Algeria). Journal of Biodiversity and Environmental Sciences, JBES, 12, 3, 226–235.

Caby R., Hammor D. 1992. Le massif cristallin de l'Edough (Algérie): un 'Metamorphic Corecomplex' d'âge miocène dans les Maghrébides. Comptes rendus de l'Académie des sciences. Série 2. Mécanique, physique, chimie, sciences de l'univers, sciences de la terre, 314 (08), 829–835.

Cao S., Duan X., Zhao X., Ma J., Dong T., Huang N., Sun C., He B., Wei F. 2014. Health Risks from the Exposure of Children to As, Se, Pb and Other Heavy Metals near the Largest Coking Plant in China. Science of the Total Environment, 472, 1001–1009.

Chen J., Huang Q., Lin Y., Fang Y., Qian H., Liu R., Ma H. 2019. Hydrogeochemical characteristics and quality assessment of groundwater in an irrigated region, Northwest China. Water, 11(1), 18.

Davies J.M. 2006. Application and Tests of the Canadian Water Quality Index for Assessing Changes in Water Quality in Lakes and Rivers of Central North America. Lake and Reservoir Management, 22, 4, 308–320. https://doi.org/10.1080/07438140609354365.

Debernardi L., De Luca D.A., Lasagna M. 2008. Correlation between nitrate concentration in groundwater and parameters affecting aquifer intrinsic vulnerability. Environmental Geology, 55, 539–558.

Debièche T.H., Mania J., Mudry J. 2003. Species and mobility of phosphorus and nitrogen in a wadi relationship. J. Afric. Earth Sci., 37/1-2/47-57.

Djabri L., Hani A., Laouar R., Mania J., Mudry J., Louhi A. 2003. Potential pollution of groundwater in the valley of the Seybouse River, north-eastern Algeria. Environmental Geology, 44, 738–744.

Djidel M. 2004. Etude hydrochimique des nappes côtières cas des nappes du littoral d'Annaba-El Kala (Nord-Est Algérien) mémoire de magistère. Univ. Annaba, 37.

Djorfi S. et al. 2008. Impacts des rejets industriels sur la qualité des eaux de l'aquifère d'Annaba (Algérie). Bull. Ser. Géol. Nat., 49.

Environmental Protection Agency (U.S.). 2017. Final Determination on the Appropriateness of the Model Year 2022–2025 Light-Duty Vehicle Greenhouse Gas Emissions Standards under the Midterm Evaluation. EPA-420-R-17-001. U.S. Environmental Protection Agency: Washington, DC, USA, January 2017.

Fan A.M. 2011. Nitrate and Nitrite in Drinking Water: A Toxicological Review California Environmental Protection Agency, Oakland.

He S., Li P. 2019. A MATLAB based graphical user interface (GUI) for quickly producing widely used hydrogeochemical diagrams. Geochemistry. https://doi.org/10.1016/j.chemer.2019.125550.

He S., Wu J. 2019. Hydrogeochemical characteristics, groundwater quality, and health risks from hexavalent chromium and nitrate in groundwater of Huanhe formation in Wuqi County, Northwest China. Expo Health, 11(2), 125–137. https://doi.org/10.1007/s1240 3-018-0289-7.

Khan R., Jhariya D.C. 2017. Groundwater quality assessment for drinking purpose in Raipur city. Chhattisgarh using water quality index and geographic information system. J. Geol. Soc. India, 90, 69–76. https://doi.org/10.1007/s12594-017-0665-0.

Khanoranga K.S. 2019. An assessment of groundwater quality for irrigation and drinking purposes around brick kilns in three districts of Balochistan province, Pakistan, through water quality index and multivariate statistical approaches. J. Geochem. Explor., 197, 14–26.

Li P., Qian H., Wu J. 2010. Groundwater quality assessment based on improved water quality index in Pengyang County, Ningxia, and Northwest China. E-J Chem., 7(S1), S209–S216. https://doi.org/10.1155/2010/45130 4.

Li P., Zhang Y., Yang N. et al. 2016c. Major ion chemistry and quality assessment of groundwater in and around a mountainous tourist town of China. Expo Health, 8(2), 239–252. https://doi.org/10.1007/s12403-016-0198-6.

Li P., Qian H., Wu J. 2018c. Conjunctive use of groundwater and surface water to reduce soil salinization in the Yinchuan plain, North-West China. Int. J. Water Resour. Dev., 34(3), 337–353.

Li P., He X., Li Y., Xiang G. 2019a. Occurrence and health implication of fluoride in groundwater of loess aquifer in the Chinese Loess Plateau: a case study of Tongchuan, Northwest China. Expos Health, 11(2), 95–107. https://doi.org/10.1007/s12403-018-0278-x.

Messadi D.V., Le A., Berg S., Jewett A., Wen Z., Kelly P., Bertolami C.N. 1999. Expression of apoptosis-associated genes by human dermal scar fibroblasts. Wound Repair and Regeneration, 7(6), 511–517.

Mohammadi A.A., Zarei A., Majidi S., Ghaderpoury A., Hashempour Y., Saghi M.H., Aline-
    jad A., Yousefi M., Hosseingholizadeh N., Ghaderpoori M. 2019. Carcinogenic and Non-
    Carcinogenic Health Risk Assessment of Heavy Metals in Drinking Water of Khorramabad,
    Iran. Methods, 6, 1642–1651. https://doi.org/10.1016/j.mex.2019.07.017.

Piper A.M. 1944. A graphic procedure in the geochemical interpretation of water-analysis.
    Trans. Am. Geophys. Union, 25(6), 914–928. https://doi.org/10.1029/TR25i 006p00914.

Qiu J. 2010. China faces up to groundwater crisis. Nature, 466(7304), 308.

Rahman M.M., Bodrud-Doza M., Siddiqua M.T., Zahid A., Islam A.R.M.T. 2020. Spatiotempo-
    ral distribution of fluoride in drinking water and associated probabilistic human health risk
    appraisal in the coastal region, Bangladesh. Science of the Total Environment, 724, 138316.

RAIS. 2017. Risk Assessment Information System in the Risk Exposure Models for Chemicals
    User's Guide. https://rais.ornl.gov/tools/rais_chemical_risk_guide.

Rezaei H., Jafari A., Kamarehie B., Fakhri Y., Ghaderpoury A., Karami M.A., Ghaderpoori
    M., Shams M., Bidarpoor F., Salimi M. 2019. Health-risk assessment related to the fluoride,
    nitrate, and nitrite in the drinking water in the Sanandaj, Kurdistan County, Iran. Hum. Ecol.
    Risk Assess., 25(5), 1242–1250.

Sanou A., Méité N., Kouyaté A., Irankunda E., Kouamé A.N., Koffi A.E., … Kouakou L.P.M.S.
    2022. Assessing levels and health risks of fluoride and heavy metal contamination in drink-
    ing water. Journal of Geoscience and Environment Protection, 10(11), 15–34.

Tepanosyan G., Maghakyan N., Sahakyan L., Saghatelyan A. 2017. Heavy metals pollution lev-
    els and children health risk assessment of Yerevan kindergartens soils. Ecotoxicology and
    Environmental Safety, 142, 257–265.

Touré A., Wenbiao D., Keita Z., Dembele A., Abdalla Elzaki E.E. 2019. Drinking Water Qual-
    ity and Risk for Human Health in Pelengana Commune, Segou, Mali. Journal of Water and
    Health, 17, 609–621. https://doi.org/10.2166/wh.2019.004.

USEPA 1989. Risk Assessment Guidance for Superfund, vol. 1: Human Health Evaluation Man-
    ual (Part A), United States Environmental Protection Agency, Washington, DC, USA.

USEPA 2010. Human Health Risk Assessment: Risk-Based Concentration Table. http://www.
    epa.gov/reg3hwmd/risk/human/rb-concentration_table/Generic_Tables.

Verma D.K., Bhunia G.S., Shit P.K. et al. 2018. Assessment of groundwater quality of the central
    Gangetic Plain area of India using geospatial and WQI Techniques. J. Geol. Soc. India, 92,
    743–752. https://doi.org/10.1007/s12594-018-1097-1.

WHO 2017. Guidelines for Drinking-Water Quality: Fourth Edition Incorporating the First Ad-
    dendum. World Health Organization, Geneva, Switzerland.

Wu J., Sun Z. 2016. Evaluation of shallow groundwater contamination and associated human
    health risk in an alluvial plain impacted by agricultural and industrial activities, mid-west
    China. Expo Health, 8(3), 311–329. https://doi.org/10.1007/s1240 3-015-0170-x.

Wu J., Wang L., Wang S., Tian R., Xue C., Feng W., Li Y. 2017. Spatiotemporal variation of
    groundwater quality in an arid area experiencing long-term paper wastewater irrigation,
    northwest China. Environ. Earth Sci., 76(13), 460. https://doi.org/10.1007/s12665-017-
    6787-2.

Xu P., Feng W., Qian H., Zhang Q. 2019a. Hydrogeochemical characterization and irrigation
    quality assessment of shallow groundwater in the Central Western Guanzhong Basin, China.
    Int. J. Environ. Res. Public Health, 16(9), 18.

Yu C., Gong P., Yin Y. 2011. China's water crisis needs more than words. Nature, 470(7334),
    307–307.

Zakir H.M., Sharmin S., Akter A., Rahman M.S. 2020. Assessment of Health Risk of Heavy
    Metals and Water Quality Indices for Irrigation and Drinking Suitability of Waters: A Case

Study of Jamalpur Sadar Area, Bangladesh. Environmental Advances, 2, 100005. https://doi.org/10.1016/j.envadv.2020.100005.

Zhang Q., Xu P., Qian H. 2020. Groundwater quality assessment using improved water quality index (WQI) and human health risk (HHR) evaluation in a semi-arid region of northwest China. Exposure and Health, 12, 487–500.

Zotou I., Tsihrintzis V.A., Gikas G.D. 2019. Performance of seven water quality indices (WQIs) in a Mediterranean River. Environ. Monit. Assess., 191(8), 505.

PhD Fenazi Bilal
Hydrocarbon and Earth Sciences Faculty
Ouargla University, 30000 Ouargla, Algeria
email: b_fenazi@yahoo.fr

PhD Boucenna Fatih
Energy and Materials Laboratory
Faculty of Sciences and Technology
Tamanrasset University, Algeria
City of Teachers 70 lgt, Tamanrasset, Algeria
email: boucennafatih@gmail.com.

Prof. Aziez Zeddouri
Hydrocarbon and Earth Sciences Faculty
Ouargla University, 30000 Ouargla, Algeria
email: zeddouriaziez@yahoo.fr.
ORCID: 0000-0001-9619-1830